Biomedical Optics EXPRESS

Optimizing light transport in scintillation crystals for time-of-flight PET: an experimental and optical Monte Carlo simulation study

Eric Berg,[1,2,*] Emilie Roncali,[1,2] and Simon R. Cherry[1]

[1]*Department of Biomedical Engineering, University of California, Davis, One Shields Avenue, Davis, CA, 95616, USA*

[2]*These authors contributed equally*

[*]*eberg@ucdavis.edu*

Abstract: Achieving excellent timing resolution in gamma ray detectors is crucial in several applications such as medical imaging with time-of-flight positron emission tomography (TOF-PET). Although many factors impact the overall system timing resolution, the statistical nature of scintillation light, including photon production and transport in the crystal to the photodetector, is typically the limiting factor for modern scintillation detectors. In this study, we investigated the impact of surface treatment, in particular, roughening select areas of otherwise polished crystals, on light transport and timing resolution. A custom Monte Carlo photon tracking tool was used to gain insight into changes in light collection and timing resolution that were observed experimentally: select roughening configurations increased the light collection up to 25% and improved timing resolution by 15% compared to crystals with all polished surfaces. Simulations showed that partial surface roughening caused a greater number of photons to be reflected towards the photodetector and increased the initial rate of photoelectron production. This study provides a simple method to improve timing resolution and light collection in scintillator-based gamma ray detectors, a topic of high importance in the field of TOF-PET. Additionally, we demonstrated utility of our Monte Carlo simulation tool to accurately predict the effect of altering crystal surfaces on light collection and timing resolution.

OCIS codes: (170.2670) Gamma ray imaging; (240.0240) Optics at surfaces; (120.3890) Medical optics instrumentation; (170.5280) Photon migration; (240.5770) Roughness; (260.1180) Crystal optics.

References and links

1. J. S. Karp, S. Surti, M. E. Daube-Witherspoon, and G. Muehllehner, "Benefit of time-of-flight in PET: experimental and clinical results," J. Nucl. Med. **49**(3), 462–470 (2008).
2. T. K. Lewellen, "Time-of-flight PET," Semin. Nucl. Med. **28**(3), 268–275 (1998).
3. W. W. Moses, "Time-of-flight in PET revisited," IEEE Trans. Nucl. Sci. **50**(5), 1325–1330 (2003).
4. E. Testa, M. Bajard, M. Chevallier, D. Dauvergne, F. Le Foulher, N. Freud, J. Letang, J. Poizat, C. Ray, and M. Testa, "Dose profiling monitoring with carbon ions by means of prompt-gamma measurements," Nucl. Instrum. Methods Phys. Res. B **267**(6), 993–996 (2008).
5. M. Conti, "Focus on time-of-flight PET: the benefits of improved time resolution," Eur. J. Nucl. Med. Mol. Imaging **38**(6), 1147–1157 (2011).
6. T. K. Lewellen, "Recent developments in PET detector technology," Phys. Med. Biol. **53**(17), R287–R317 (2008).
7. D. Renker, "New trends of photodetectors," Nucl. Instrum. Methods Phys. Res. A **571**(1-2), 1–6 (2007).
8. M. Conti, L. Eriksson, H. Rothfuss, and C. L. Melcher, "Comparison of fast scintillators with TOF PET potential," IEEE Trans. Nucl. Sci. **56**(3), 926–933 (2009).
9. P. Lecoq, E. Auffray, S. Brunner, H. Hillemanns, P. Jarron, A. Knapitsch, T. Meyer, and F. Powolny, "Factors influencing time resolution of scintillators and ways to improve them," IEEE Trans. Nucl. Sci. **57**(5), 2411–2416 (2010).

#236602 - $15.00 USD Received 23 Mar 2015; revised 16 May 2015; accepted 19 May 2015; published 26 May 2015

10. S. E. Brunner, L. Gruber, J. Marton, K. Suzuki, and A. Hirtl, "Studies on the Cherenkov effect for improved timing resolution of TOF-PET," IEEE Trans. Nucl. Sci. **61**(1), 443–447 (2014).
11. P. Lecoq, E. Auffray, and A. Knapitsch, "How photonic crystals can improve the timing resolution of scintillators," IEEE Trans. Nucl. Sci. **60**(3), 1653–1657 (2013).
12. C. Degenhardt, G. Prescher, T. Frach, R. de Gruyter, A. Schmitz, and R. Ballizany, "The digital silicon photomultiplier – a novel sensor for the detection of scintillation light," IEEE NSS-MIC Conference Record, N28–5 (2009).
13. P. Lecoq, "New approaches to improve timing resolution in scintillators," IEEE Trans. Nucl. Sci. **59**(5), 2313–2318 (2012).
14. V. Ch. Spanoudaki and C. S. Levin, "Investigating the temporal resolution limits of scintillation detection from pixellated elements: comparison between experiment and simulation," Phys. Med. Biol. **56**(3), 735–756 (2011).
15. W. W. Moses and S. E. Derenzo, "Prospects for time-of-flight PET using LSO scintillator," IEEE Trans. Nucl. Sci. **46**(3), 474–478 (1999).
16. S. E. Derenzo, W.-S. Choong, and W. W. Moses, "Fundamental limits of scintillation detector timing precision," Phys. Med. Biol. **59**(13), 3261–3286 (2014).
17. L. G. Hyman, "Time resolution of photomultiplier systems," Rev. Sci. Instrum. **36**(2), 193–196 (1965).
18. E. Roncali and S. R. Cherry, "Simulation of light transport in scintillators based on 3D characterization of crystal surfaces," Phys. Med. Biol. **58**(7), 2185–2198 (2013).
19. E. Roncali, J. P. Schmall, V. Viswanath, E. Berg, and S. R. Cherry, "Predicting the timing properties of phosphor-coated scintillators using Monte Carlo light transport simulation," Phys. Med. Biol. **59**(8), 2023–2039 (2014).
20. S. Seifert, J. H. L. Steenbergen, H. T. Dam, and D. R. Schaart, "Accurate measurement of the rise and decay times of fast scintillators with solid state photon counters," J. Instrum. **7**(9), P09004 (2012).
21. Q. Fang, T. Papaioannou, J. A. Jo, R. Vaitha, K. Shastry, and L. Marcu, "Time-domain laser-induced fluorescence spectroscopy apparatus for clinical diagnosis," Rev. Sci. Instrum. **75**(1), 151–162 (2004).
22. M. Janecek and W. W. Moses, "Optical reflectance measurements for commonly used reflectors," IEEE Trans. Nucl. Sci. **55**(4), 2432–2437 (2008).
23. H. Rothfuss, M. Casey, M. Conti, N. Doshi, L. Eriksson, and M. Schmand, "Monte Carlo simulation study of LSO crystals," IEEE Trans. Nucl. Sci. **51**(3), 770–774 (2004).

1. Introduction

Scintillator-based gamma ray detectors with excellent timing resolution are becoming increasingly important to enhance performance of nuclear medicine systems such as positron emission tomography (PET). In PET, there is currently a trend toward using TOF to improve signal-to-noise ratio of reconstructed images [1]. TOF allows localization of annihilation events along lines of response by measuring the arrival time difference of the two 511 keV annihilation photons, with a precision determined by the detector timing resolution [2,3]. Although the current achievable timing resolution (~400 ps) is insufficient for direct reconstruction from TOF data, TOF-PET has been shown to increase image signal-to-noise and thus improve lesion detectability [1]. TOF information has also been used to estimate the mass of an interacting particle based on its speed, to identify types of interacting radiation, or to verify range in proton therapy [4]. As further improvements in detector timing resolution will lead to superior performance [5], a variety of approaches to improve timing resolution are under investigation [6–12].

A scintillation detector is typically composed of a scintillator crystal that converts incoming gamma photons (energy typically 100 – 600 keV) into visible light, coupled to a photodetector which should efficiently collect scintillation light. State-of-the-art commercial PET detectors typically employ lutetium-based scintillators (e.g. lutetium (yttrium) oxyorthosilicate L(Y)SO) and photomultiplier tubes (PMTs). Among the numerous factors affecting timing resolution of a scintillator-based gamma detector, the major contribution comes from the light transport in the scintillator and light collection by the photodetector. Light transport and collection is determined by (1) intrinsic scintillation properties (brightness, rise and decay times), (2) optical properties of the scintillator (absorption and scattering, surface finish, and external reflector), and (3) photodetector characteristics (quantum efficiency, noise, and timing properties). With modern photodetectors, the scintillator is the main limiting factor in the timing resolution. The scintillator's intrinsic timing resolution is primarily determined by the rate at which photoelectrons are produced and collected in the first nanosecond [13], which is governed by both the intrinsic scintillator emission and optical properties. Given the high index of refraction of most inorganic crystal scintillators (typically 1.5 – 2.1), the surface finish contributes significantly to the light

#236602 - $15.00 USD Received 23 Mar 2015; revised 16 May 2015; accepted 19 May 2015; published 26 May 2015

transport in the crystal, because of internal reflections and large refraction angles. Improving the timing resolution can thus only be achieved by optimizing every aspect of the light transport.

It has been shown that for high aspect-ratio crystals (thick crystals with small cross section) read out by a single photodetector at one end, mechanically polished or chemically etched surfaces provide superior light collection and timing resolution compared to rough (as-cut or ground) surfaces, due to improved light transport towards the readout end of the crystal [14,15]. In a recent study, the impact of numerous factors affecting timing resolution (scintillator luminosity, rise and decay time, photodetector properties, etc.) were characterized in an exhaustive Monte Carlo study to obtain lower limits of timing resolution over a range of these parameters [16]. However, these studies only considered surface finishes that were uniformly applied to all crystal surfaces (typically all polished surfaces), and provided only limited description of the light transport, which made them unable to accurately predict timing resolution in other configurations. Our experimental data from a recent study showed that when only a section of one polished crystal surface was roughened, both light collection and timing resolution improved. Interestingly, the observed timing resolution improvement did not agree with predictions from theoretical models describing the statistical relationship between light collection and timing resolution [17]. Here, we aim to comprehensively characterize changes in light collection and timing resolution with partially roughened crystals compared to completely polished surfaces. Our optical Monte Carlo tool designed specifically for optical modeling of scintillator crystals, including timing properties, was used to gain further understanding into changes in light transport for roughened crystals and to explain observed changes in timing resolution not predicted by previous theoretical models.

2. Materials and methods

2.1 Crystal surface treatment

3.34 x 3.34 x 20 mm^3 mechanically polished cerium-doped lutetium yttrium oxyorthosilicate (LYSO:Ce) scintillator crystals (Crystal Photonics Inc., Sanford, Florida) were used in this study. Polished surfaces were roughened using a compact, custom-built mill with a diamond burr (500 grit). The roughening length was manually chosen while the milling depth was set to 50 μm.

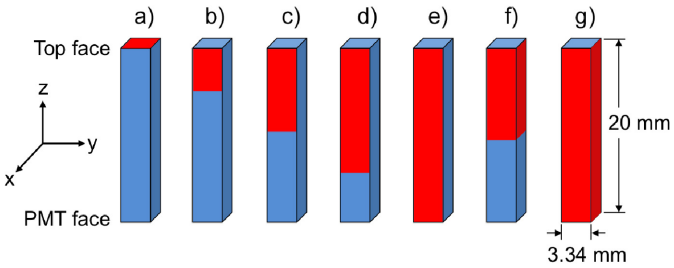

Fig. 1. Surface roughening sections are indicated by red, polished surfaces by blue. a) Top surface roughened, b) – e) One side roughened 5 – 20 mm, f) Two sides roughened 10 mm, g) All lateral sides roughened 20 mm. The bottom surface of the crystal is coupled to the PMT.

Seven roughening configurations were investigated (Fig. 1). The same crystal was used for roughening configurations b)-e) and g) and so three crystals were used. All crystals were measured before roughening so that any changes in light output and timing resolution were a result of surface roughening, rather than crystal variability. All experiments with a particular crystal were performed under the same conditions (temperature, photodetector parameters).

#236602 - $15.00 USD Received 23 Mar 2015; revised 16 May 2015; accepted 19 May 2015; published 26 May 2015

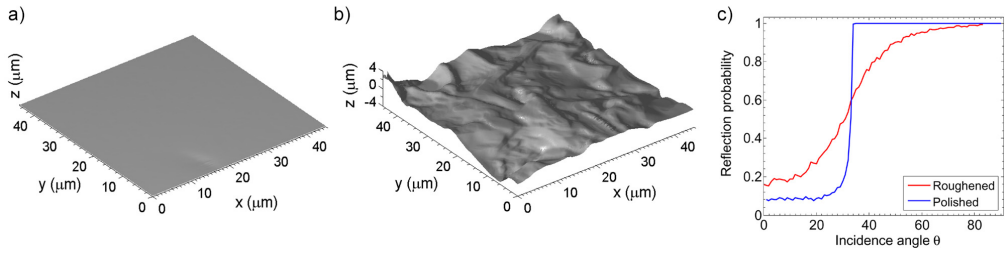

Fig. 2. a) AFM sample of polished surface. b) AFM sample of roughened surface. c) Computed reflectance curves for polished and roughened sections.

The surface 3D topography was assessed using atomic force microscopy (AFM) on both polished (Fig. 2(a)) and roughened (Fig. 2(b)) crystals. 45 μm x 45 μm samples were acquired with a spatial resolution of 90 nm, on separate crystals that received the same surface treatment. For the polished crystal, the average roughness (Ra), rms roughness (σ), and peak-to-valley ratio (Rpv) were 17.7 nm, 25.7 nm, and 68.9 nm. In contrast, Ra, σ, and Rpv were 1 μm, 1.28 μm, and 6.2 μm for the rough crystal (note the different scales). In particular, Rpv highlights the non-uniformity of the rough surface that shows high peaks and deep valleys.

2.2 Experimental characterization of the scintillation crystals

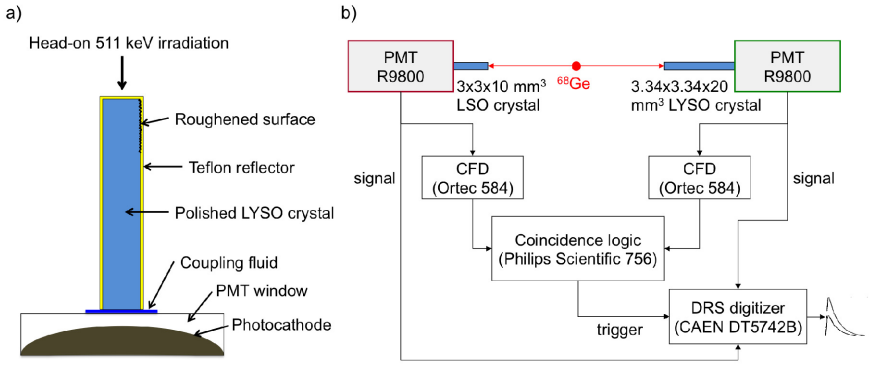

Fig. 3. a) Schematic used for testing crystals. Drawing is not to scale. A light absorbing material (not shown) is placed around the crystals outside the reflector to secure the crystals to the PMT window. b) Experimental setup used to acquire detector data.

The crystals were wrapped with three layers of Teflon tape and coupled to the center of fast, single-channel photomultiplier tubes (PMT R9800, Hamamatsu Photonics K. K.) via silicon optical coupling fluid (BC-630, Bicron) as shown in Fig. 3(a). The refractive indices of the crystal, coupling fluid, and the borosilicate glass PMT window were 1.82, 1.45 and 1.5 respectively. The crystals were tested as shown in Fig. 3(b). All experiments were performed in a light-tight enclosure. A reference detector (3 x 3 x 10 mm^3 polished LSO crystal coupled to a R9800 PMT) was used to select coincidence pairs of 511 keV photons. Five measurements were taken with each roughening configuration, each containing 50,000 coincident events, by digitizing the light pulses at 5 GS/s with a 12-bit 16-channel DRS-based digitizer. The crystals were re-coupled to the PMT window between each measurement. Experiments were performed with a ^{68}Ge (320 kBq) point source. Signal post-processing was performed offline.

2.3 Signal analysis: computation of light collection and timing resolution

The amount of scintillation light collected by the photodetector was determined by integrating each pulse over 120 ns. The integral values were histogrammed into energy spectra fitted with a Gaussian distribution. The position of the 511 keV photopeak extracted from the Gaussian

#236602 - $15.00 USD Received 23 Mar 2015; revised 16 May 2015; accepted 19 May 2015; published 26 May 2015

fit was used as the light collection metric. Energy resolution was computed as the ratio between the fit FWHM and peak position and expressed as a percentage. Only events with computed energy values between 425 – 650 keV were used for timing resolution analysis. The timing pick-off for each pulse was determined as the time that the signal's leading edge crosses a set threshold. Timing pick-off values were obtained over a range of thresholds to find the threshold that gave the best timing resolution for each roughening configuration. FWHM timing resolution values were extracted from a Gaussian fit applied to histogrammed timing data. Coincidence timing resolution for an identical pair of the detector under test was found by subtracting in quadrature the contribution of the reference detector (220 ps) from the measured timing resolution and multiplying by √2 [15].

2.4 Optical Monte Carlo simulations

Accurately modeling light transport in scintillator crystals is challenging because reflectance properties of crystal surfaces are difficult to describe. As a result, the numerous existing Monte Carlo simulation tools used in nuclear medicine do not accurately predict light transport except for optically polished surfaces. Raytracing software such as Zemax offer sophisticated options to model rough surfaces, however, they do not allow detailed recording of the photon timing properties, which is crucial to accurately model the detector timing resolution. To address this shortcoming, we have developed a Monte Carlo simulation tool that models scintillation light production, transport in the crystal, and detection by various types of photodetectors. Detailed description and validation of our simulation tool can be found in [18,19]. Here, we extend our previous work to include coupling to a photodetector defined by its quantum efficiency, single photon pulse response, and noise properties. Following the generation of scintillation photons in the crystal, described by a bi-exponential distribution (rise time 72 ps and decay time 42 ns [20,21]), each photon was tracked within the scintillator until it was either absorbed, escaped, or entered the PMT (Fig. 4). The quantum efficiency spectrum of the PMT was used to determine whether an incident photon would ultimately generate a photoelectron. The total distance traveled by photons detected by the PMT was used to compute the transit time using the speed of light in LYSO. Photoelectron generation times are the sum of the 511 keV gamma travel time, scintillation emission time, and photon transit time.

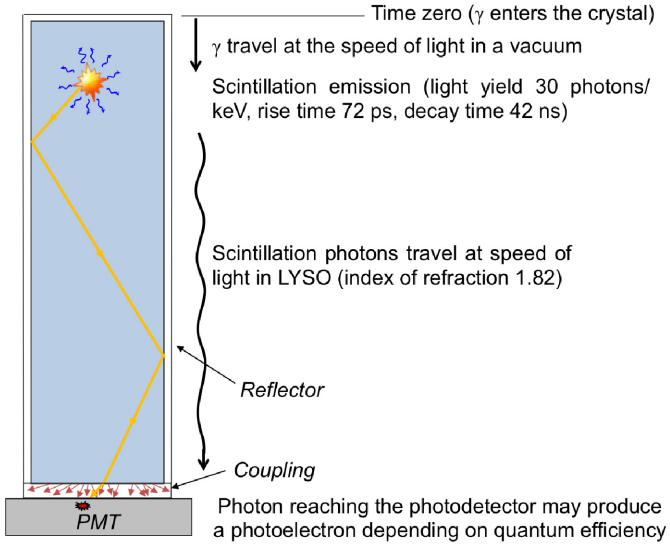

Fig. 4. Processes involved in generating simulated scintillation pulses.

#236602 - $15.00 USD Received 23 Mar 2015; revised 16 May 2015; accepted 19 May 2015; published 26 May 2015

A key aspect of our approach is using 3D measurements of actual crystal surfaces (obtained by AFM) to compute the reflectance properties for scintillation photon incidence angles varying from 0° to 90° (Fig. 2(c)). Our approach is comparable to bidirectional scattering distribution function (BSDF) but presents the advantage of covering all incidence angles without requiring a specific setup. The angular distributions of reflectance and reflected rays were then stored in look-up tables (LUTs) to be incorporated in the simulation code to model reflections on the crystal faces [18]. In contrast to the polished surface, which has a reflectance curve that closely follows the trend for an ideal polished surface, the roughened surface exhibits a "smoothed" reflectance curve (Fig. 2(c)). In configurations where a diffuse reflector was attached to the surface with a 30 micron air gap, three layers of Teflon tape were modeled as a Lambertian reflector with a reflection coefficient of 0.97 [22,23].

The single photon response of the R9800 PMT was extracted from ~500 experimental dark pulses (thermionic emission) by applying a Gaussian fit to the output signal. A rise time of ~1 ns was measured for the Gaussian fit. A dark count rate of ~20 kHz was measured, and was used as a noise source in the simulations (electronic noise was not modeled). Both rise time and dark count rate were consistent with the manufacturer's information. Time pick-offs for both simulated and experimental pulses were computed using the same post-processing algorithm described previously. Coincidence timing resolution was computed similarly to experimental data; the detector of interest was assumed to be in coincidence with a reference detector described by the experimental parameters. The timing resolution of the simulated reference detector was found to be 190 ps, consistent with the experimental reference detector. Simulations were performed three times for each surface configuration (Fig. 1) with 1000 counts contained in each simulation.

3. Results and discussion

3.1 Light collection

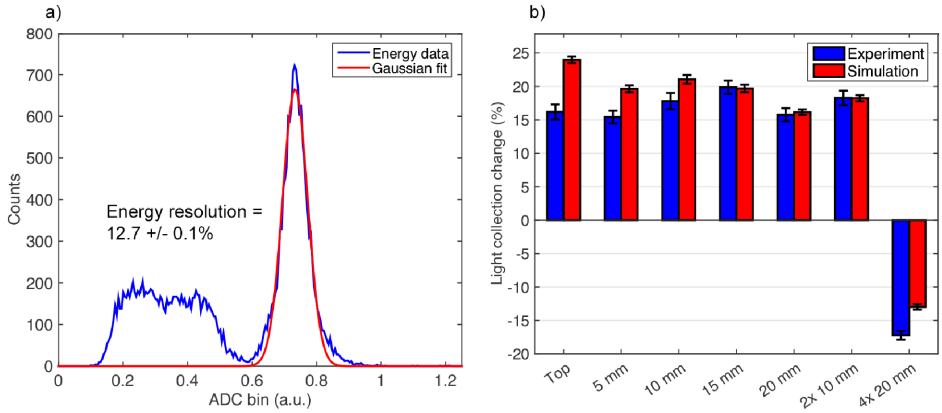

Fig. 5. a) Experimental 511 keV energy spectrum with Gaussian fit of the photopeak to estimate light collection. b) Changes in photopeak position for roughened crystals relative to all polished surfaces. Error bars represent standard deviation of five measurements for experimental data and three measurements for simulated data.

The effect of surface roughening on scintillation light collection efficiency was evaluated by measuring the position of the 511 keV photopeak (Fig. 5(a)), and characterizing changes relative to polished crystals. With the exception of the crystal with all lateral sides roughened (4x 20 mm), all roughened crystals showed increased light collection (Fig. 5(b)). Experimentally, the largest increase (20%) was observed with the crystal roughened 15 mm on one side, while in simulation, roughening the top surface increased the light collection by the largest amount (25%). Experimental and simulated data are generally in good agreement,

#236602 - $15.00 USD Received 23 Mar 2015; revised 16 May 2015; accepted 19 May 2015; published 26 May 2015

with the largest discrepancy apparent with the top roughened crystal. This is likely due to a combination of factors. First, when examining the light output experimentally and with simulations without a surrounding reflector, we found that the changes in light collection (relative to a polished crystal without reflector) were 3% and 15% respectively. This shows that the reflector might not be properly modeled for this face. Experimentally, Teflon tape is not folded on the small top surface in exactly three layers, rather twisted, thus light transmitted through the first layer is more likely to be trapped between subsequent layers or escape the reflector, decreasing the overall reflectivity. However this is not the only factor and does not explain all the discrepancy. Second, we observed a slight taper on the edges of the top surface that is probably caused by the roughening process: the small face of the crystal is pushed against the diamond burr instead of being gently slid as it is for roughening the lateral sides. It is beyond the scope of this paper to model a tapered crystal, but we will further investigate further this phenomenon and will also improve the roughening process for the top face.

In simulations, energy resolution for the polished crystal was 12% and varied from 10 to 13% for different roughening configurations. Again, close agreement with experimental data was obtained as the energy resolution for the polished crystal was 12.7% and values ranged from 12.5 to 16% for the roughening configurations.

3.2 Timing resolution

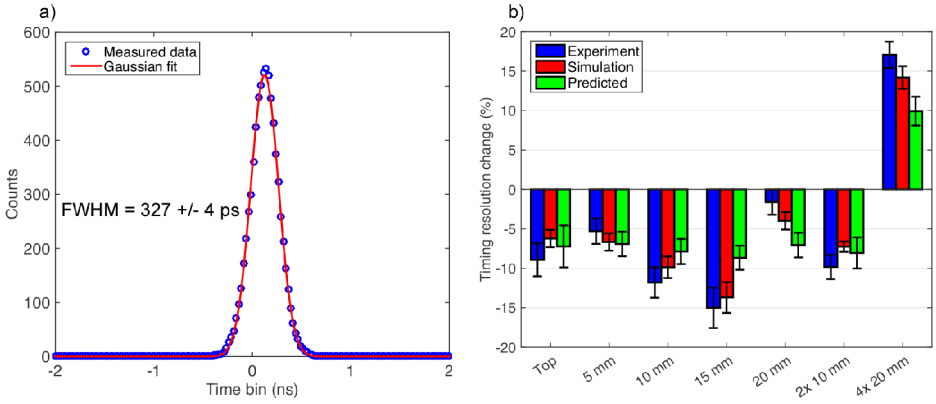

Fig. 6. a) Histogram of experimental timing data and Gaussian fit used to calculate the timing resolution. b) Changes in timing resolution with roughened surfaces relative to all polished surfaces. Error bars represent standard deviation of five measurements for experimental data and three measurements for simulated data. The green bars represent predicted changes in experimental timing resolution based on Eq. (1).

Timing resolution was calculated for each surface roughening configuration, for both experimental and simulated data using timing spectra (Fig. 6(a)). Changes in timing resolution for roughening configurations relative to all polished surfaces were computed (Fig. 6(b)). For the polished crystal, the experimental and simulated coincidence timing resolutions were 327 +/– 4 ps and 321 +/– 2 ps, respectively. Roughening 15 mm on one side provided the best timing resolution both experimentally (279 +/– 8 ps) and in simulation (277 +/– 8 ps). Simulations and experimental characterization showed very good agreement in changes in timing resolution, with an average discrepancy of 2%. The largest discrepancy was apparent with the crystal roughened on all lateral sides (4x 20 mm).

With both approaches, no direct correlation between light collection and timing resolution was observed. Using theoretical models for timing resolution based on light collection [17], predicted changes in experimental timing resolution are computed using Eq. (1):

#236602 - $15.00 USD Received 23 Mar 2015; revised 16 May 2015; accepted 19 May 2015; published 26 May 2015

$$CTR_{rough,pred} = CTR_{pol}\sqrt{\frac{N_{pol}}{N_{rough}}} \quad (1)$$

Where N denotes light collection and CTR denotes coincidence timing resolution. The predicted values (green bars in Fig. 6(b)) clearly do not correlate well with measured changes in timing resolution, therefore further analysis into the light transport in the crystal was needed to explain changes in timing resolution with partially roughened surfaces. We used Monte Carlo simulations to address these questions and access information that is not available with experimental data, focusing on the configurations that showed improvement in timing resolution with respect to the polished crystal (top roughened, 1 side 5 mm and 15 mm).

3.3 Study of light collection: angular distribution of scintillation photons

We first studied how surface roughening affected the angular distribution of the scintillation photons and could ultimately enhance light collection efficiency. In particular, the polished crystal, top surface roughened (which showed the highest improvement in light collection), one side roughened 5 mm, and one side roughened 15 mm were studied. 10,000 scintillation photons were generated at the center of the crystal (x,y), 18 mm from the PMT face (i.e. 2 mm from the top face). For the lateral side, where the surface treatment was altered on some configurations (normal vector = **x**), all directions of reflected photons were stored independently from their location and ultimate fate, and were plotted on a unit sphere (Fig. 7). Photons may be counted several times, as they undergo multiple reflections.

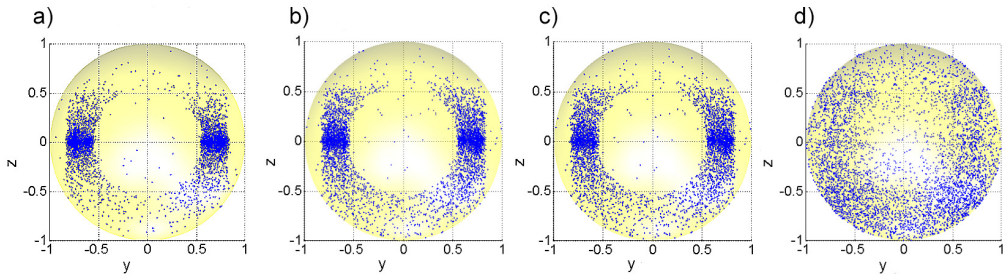

Fig. 7. Spatial distribution of photons reflected off one lateral surface for a) polished (Media 1), b) top roughened (Media 2), c) one side roughened 5 mm (Media 3), and d) one side roughened 15 mm (Media 4). Photon directions (blue points) were projected on a unit sphere (yellow).

For the polished crystal, very few reflections occurred in the 33° cone corresponding to the critical angle with this face (visible as a circle of radius equal to sin 33°). The corresponding cones for other faces were also visible (Fig. 7 and supplemental data). The polished crystal concentrated reflections in horizontal planes ($-0.15 < z < 0.15$), which indicates that these photons have to undergo multiple reflections on the four lateral sides before arriving at the bottom face coupled to the PMT. In contrast, roughening only the top face (lateral sides are still polished) changed the reflection pattern: the 33° cone is still visible, but the reflections were clearly redirected toward the bottom face ($z < 0$). This decreased the overall number of photon reflections, which (1) decreased their chance of escaping the crystal through the sides and (2) reduced the time for them to reach the bottom face that is coupled to the PMT. Roughening one lateral side 5 mm created a similar pattern, while 15 mm of roughening broadly distributed the reflections. Histograms of the angles of reflected photons from the surface normal were plotted for each of these surface configurations (Fig. 8(a)). Consistent with what is seen visually in the scatter plots, the roughened crystals show a strong bias for reflecting photons toward the PMT, as well as towards the top of the crystal, and clearly demonstrate that partial roughening of the surfaces decreased the number of photons "trapped" in horizontal planes when all surfaces were polished.

#236602 - $15.00 USD Received 23 Mar 2015; revised 16 May 2015; accepted 19 May 2015; published 26 May 2015

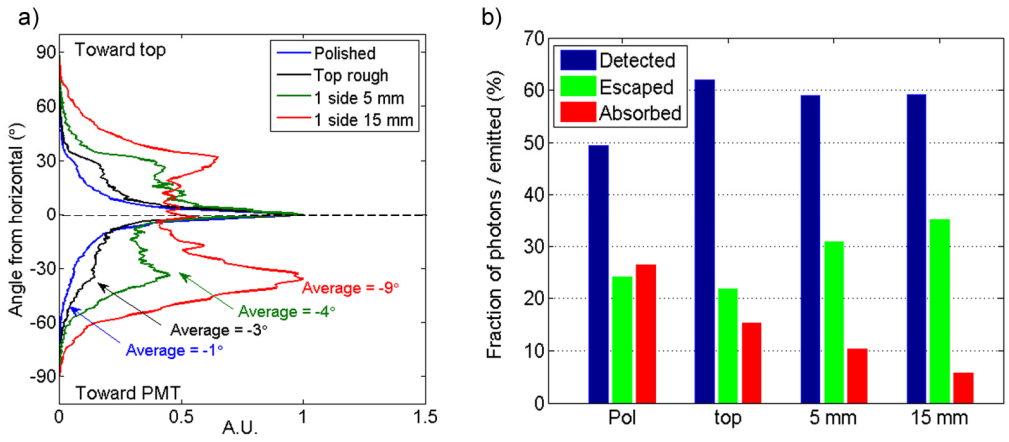

Fig. 8. a) Angles of photons reflected off crystal faces (face in contact with PMT not included). Angles were computed with respect to the horizontal assuming the crystal was vertical. b) Fraction of emitted photons that were detected, escaped through the sides of the crystal, or were absorbed (bulk absorption with absorption length = 800 mm) varied with roughening.

However two opposite effects are involved in the light collection: while surface roughening redirected more photons towards the photodetector and decreased the number of reflections, which in turn decreased the absorption (in red Fig. 8(b)), it also resulted in greater light loss through the crystal sides (in green Fig. 8(b)). The global light collection with only the top surface roughened is greatest (Fig. 5(b)) because although the number of photons that escape is similar to the polished crystal, the number of absorbed photons is significantly decreased. Roughening the lateral sides increases the number of escaping photons which counteracts the positive effect of the photon reflection pattern leading to fewer absorbed photons, as shown with the crystals roughened on one side 5 mm and 15 mm. Specifically, the crystal with one side roughened 5 mm showed lower absorption than the top roughened crystal (10% and 15% respectively) but the fraction of escaped photons was higher (31% and 22%), which ultimately resulted in slightly lower light collection (in blue) with 5 mm roughened than top roughened. Figure 8(b) also showed that roughening 5 mm or 15 mm on one side produced similar light collection, but that the light loss was not arising from the same source: 5 mm had 10% photons absorbed and 31% escaped whereas 15 mm had only 6% absorbed and 35% escaped. This might be a factor in explaining the differences in timing resolution.

3.5 Simulation study of timing resolution

In PET, timing resolution typically relies on the earliest photoelectrons generated in the PMT, which explains the weak correlation between the total light collection and the timing resolution. Each of these early photoelectrons is characterized by a generation time that is the sum of the gamma photon path length in the crystal, the scintillation emission, and the transit time of scintillation light in the crystal. To understand how the roughening altered timing resolution, we studied the distribution of the early photoelectron time stamps and the coincidence timing resolution with simulations. Only scintillation events occurring 18 +/– 1.5 mm from the PMT face (i.e. 2 mm from top surface) were used, as the variation of light transport in the crystal will be greatest here between roughening configurations.

#236602 - $15.00 USD Received 23 Mar 2015; revised 16 May 2015; accepted 19 May 2015; published 26 May 2015

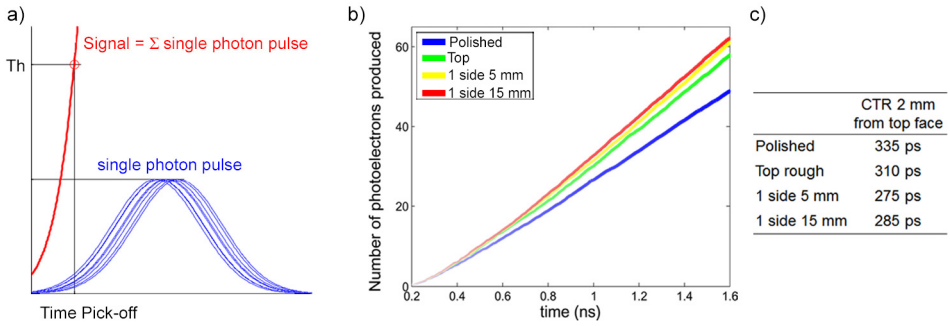

Fig. 9. a) Schematic representation of computing signals from single photon responses. For each photoelectron, a Gaussian pulse is generated (blue), and the sum of all Gaussian pulses forms the signal (red). With a 1 ns rise time, the sum of single photon responses quickly reaches the timing pick-off threshold (Th). b) Photoelectron production rate for 4 surface configurations, showing that the crystals with one side roughened 5 mm and 15 mm produced more photoelectrons around the pick-off time (~1.3 ns). c) Coincidence timing resolution for the 200 events used for photoelectron production rate analysis.

Each photoelectron produces a "single photon response" centered on its time stamp, with a 1 ns rise rime Gaussian shape measured for the PMT used in our experiments (Fig. 9(a)). The sum of these single photon responses forms the signal used to pick-off a time at a desired threshold. Figure 9(a) shows that such a pulse shape makes the leading edge of the pulse increase very rapidly, because of the long tails of the Gaussian responses. On average, simulated timing pick-off values were ~1.3 ns and 25-60 photoelectrons were required for the pulse to reach the threshold (Th). This number depends on the distribution of the photoelectron time stamps: with more photoelectrons produced in a short period of time, the threshold is reached earlier and the spread of the timing pick-off values is lowered. For the different surface configurations, we computed the coincidence timing resolution using 200 events generated 18 +/– 1.5 mm from the PMT face (i.e. 2 mm from the entrance surface), and studied the production rate of photoelectrons for these same 200 events. Figure 9(b)-9(c) shows the correlation between timing resolution and average photoelectron production rate. Consistent with our previous timing resolution results, the polished crystal provided the poorest timing resolution (335 ps) and clearly the photoelectron production rate was lower than the other configurations. The slope of the curves generally correlated with the timing resolution, except for the one side roughened 5 mm and 15 mm configurations. However, the timing resolutions obtained with these two configurations only varied by 10 ps. When the standard deviation between the 200 events (represented by the width of the lines in Fig. 9(b)) and the timing resolution uncertainty (~5 ps) are included, there was no significant difference between these two configurations around the time pick-off of 1.3 ns.

We further studied factors impacting the photoelectron production rate, such as the emission times and the scintillation light transit times. No differences were observed that could explain the subtle variations in coincidence timing resolution, demonstrating that the numerous statistical phenomena affecting the timing properties cannot be separated and that a complete model of the light transport in the crystal and the photodetector response is necessary to predict timing resolution.

4. Conclusion

Experiments and simulations showed that light collection increased and timing resolution improved when select sections of an otherwise polished crystal were roughened. The largest improvement in timing resolution, approximately 15%, was observed when a 15 mm length section of one lateral surface was roughened. Although it has been shown before that ground or chemical etched surfaces could improve timing resolution, the underlying mechanisms were not fully understood, which made it impossible to derive tools or rules to accurately predict timing resolution in scintillation detectors. The main goal of this paper was to explain

#236602 - $15.00 USD Received 23 Mar 2015; revised 16 May 2015; accepted 19 May 2015; published 26 May 2015

the experimental results we obtained using optical Monte Carlo simulations. We extended a custom Monte Carlo tool that we previously developed to accurately model light transport in scintillators with any type of surface treatment (roughness), and obtained excellent agreement between experimental and simulation results for all configurations, demonstrating the ability of the model to predict detector timing resolution, which will allow more rapid development of high performance detectors by reducing the parameter space for experimental testing.

We used the model to explain the differences in light collection we observed between the different surface treatments, and further studied timing properties as well. We showed that our model was able to predict subtle differences in photoelectron production rates. An important finding of this study is that every component of the light transport in the crystal and photodetector affects the timing resolution, and that it is impossible to completely separate these factors. One example is the light path in the crystal (and subsequent transit time), and the scintillation emission; photons that are emitted early may travel for a long time in the crystal and produce photoelectrons later or even escape the crystal, whereas later scintillation photons may be detected early if their travel time is short. A second example is the effect of the photodetector response on the rising edge of the signal used for timing pick-off.

The results of this study provide a simple method for improving timing resolution of scintillator-based gamma detectors, such as those used for TOF-PET, simply by roughening sections of the polished crystal surfaces. Although this study focused solely on LYSO, and is therefore most directly applicable for PET detectors, the changes in light transport induced by surface roughening could be studied with our simulation model for any scintillator. However, the optimal combination of roughened and polished surfaces will likely by strongly dependent on the crystal's aspect ratio and the scintillation properties. Future studies will also focus on the reflector attached to the crystal surface to further optimize light transport.

Acknowledgments

Funding for this work was provided by a Research Investments in Science and Engineering grant from UC Davis, by NIH grant R01 CA170874 and a Natural Sciences and Engineering Research Council Postgraduate Fellowship (E.B.). The authors would like to thank other members of the laboratory for helpful discussions related to this work.